Materials and Design 88 (2015) 398–405

Contents lists available at ScienceDirect

Materials and Design

journal homepage: www.elsevier.com/locate/jmad

Cryorolling effect on microstructure and mechanical properties of Fe–25Cr–20Ni austenitic stainless steel

Yi Xiong [a,b,*], Tiantian He [c], Junbei Wang [a], Yan Lu [a], Lufei Chen [a], Fengzhang Ren [a,b], Yuliang Liu [a], Alex A. Volinsky [d]

[a] School of Materials Science and Engineering, Henan University of Science and Technology, Luoyang 471023, China
[b] Collaborative Innovation Center of Nonferrous Metals, Luoyang 471023, China
[c] Institute of Metal Research, Chinese Academy of Sciences, Shenyang 110016, China
[d] Department of Mechanical Engineering, University of South Florida, Tampa, FL 33620, USA

ARTICLE INFO

Article history:
Received 24 April 2015
Received in revised form 26 July 2015
Accepted 7 September 2015
Available online 11 September 2015

Keywords:
Austenitic stainless steel
Cryorolling
Microstructure
Mechanical properties

ABSTRACT

Microstructure and mechanical properties of the Fe–25Cr–20Ni austenitic stainless steel after cryorolling with different reductions were investigated by means of optical, scanning and transmission electron microscopy, X-ray diffraction and mini-tensile testing. High density tangled dislocations and a small amount of deformation twins formed after 30% deformation. After 50% strain, a large amount of deformation twins was generated. Meanwhile, interactions between the twins and dislocations started to happen. As the strain increased to 70%, many deformation twins were produced and the interactions between the twins and dislocations were significantly enhanced. When the cryorolling was 90%, the grain size was refined to the nanometer scale. XRD analysis indicated that the diffraction peaks of the samples became broader with the strain increase. The yield strength and the ultimate strength increased from 305 MPa and 645 MPa (before deformation) to 1502 MPa and 1560 MPa (after 90% deformation), respectively. However, the corresponding elongation decreased from 40.8% to 6.4%. The tensile fracture morphology changed from typical dimple rupture to a mixture of quasi-cleavage and ductile fracture. After 90% deformation, the microhardness was 520 HV, which increased by 100% compared with the original un-deformed sample.

1. Introduction

Austenitic stainless steels are widely used in chemical and petrochemical industry due to their excellent toughness, plasticity and corrosion resistance. Since austenitic stainless steels have relatively low strength, cold work hardening is used to meet requirements for practical applications. Most studies have shown that obvious work hardening occurs during the cold working process due to the deformation-induced martensitic transformation [1–3]. The amount of the martensite phase increases with deformation, along with the hardness and strength. Recent studies focus on austenitic stainless steels with metastable microstructure [4–6], where the martensitic transformation often occurs during deformation. However, there are few reports dealing with microstructure and mechanical properties of austenitic stainless steels, since martensitic transformation does not take place during deformation.

Dynamic recovery often occurs in the deformed structures during traditional cold working processes with the increased deformation resistance at higher strain, so the requirements for processing equipment are quite high. Decreasing the deformation temperature leads to suppression of dynamic recovery (since recovery processes are thermally activated), resulting in higher defects density and consequently higher strength [7]. Cryorolling has been applied by many researchers for producing ultra-fine-grained Al, Ni, Cu, Ti and their alloys with the aim of increasing strength [8–12]. Compared with traditional room temperature rolling, the effect of the grain refinement is greatly improved by cryorolling. The reports of cryorolling are limited for the nonferrous metals and only a few studies are devoted to the microstructure and mechanical properties of austenitic stainless steels after cryorolling. In the present paper, the effects of cryorolling with different deformations on the microstructure and mechanical properties of the Fe–25Cr–20Ni austenitic stainless steel have been studied. The results discussed in this paper can provide useful experimental support for the development and applications of the ultrafine/nano-grained austenitic stainless steels.

2. Materials and experimental procedure

2.1. Materials

A vacuum induction furnace was used to manufacture the investigated 150 kg steel ingot with the following chemical composition

* Corresponding author at: School of Materials Science and Engineering, Henan University of Science and Technology, Luoyang 471023, China.
E-mail address: xy_hbdy@163.com (Y. Xiong).

http://dx.doi.org/10.1016/j.matdes.2015.09.029

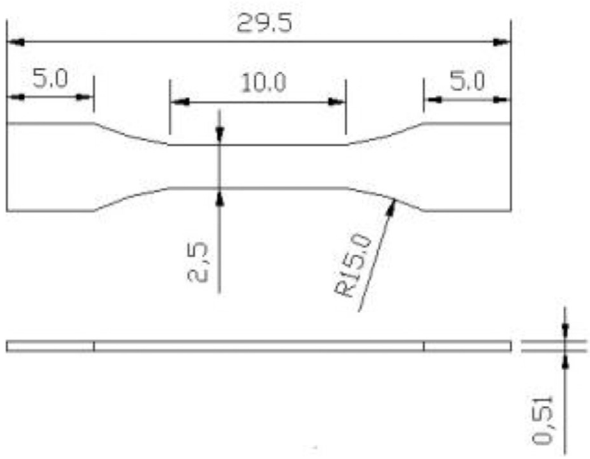

Fig. 1. The dimensions of the mini-tensile sample.

(in wt.%): 0.06C, 0.3Si, 0.6Mn, 0.02P, 0.005S, 25Cr, 20Ni, 0.25N, 0.5Nb and balance Fe. After electrical slag re-melting (ESR) process, the 120 kg ingot was hot forged down to a 5 mm thick slab. The slab was then heat treated at 1230 °C for 45 min, followed by water cooling to room temperature, and cryorolling was conducted shortly after the sample preparation.

The multi-pass unidirectional cryorolling was carried out in the two-high rolling mill. The strip was rolled by about 10% reduction at each pass, and the deformation was 30%, 50%, 70% and 90%, respectively. The samples were cryorolled after immersing them in liquid nitrogen for about 10–15 min before each pass. The cryo-rolling temperature ranged from −130 °C to −90 °C.

2.2. Experimental procedure

The microstructure characterization was carried out using optical microscopy (OLYMPUS PMG3), scanning electron microscopy (SEM, JSM-5610LV) and transmission electron microscopy (TEM, JEM-2010). For metallographic examination, samples were prepared by electrolytic

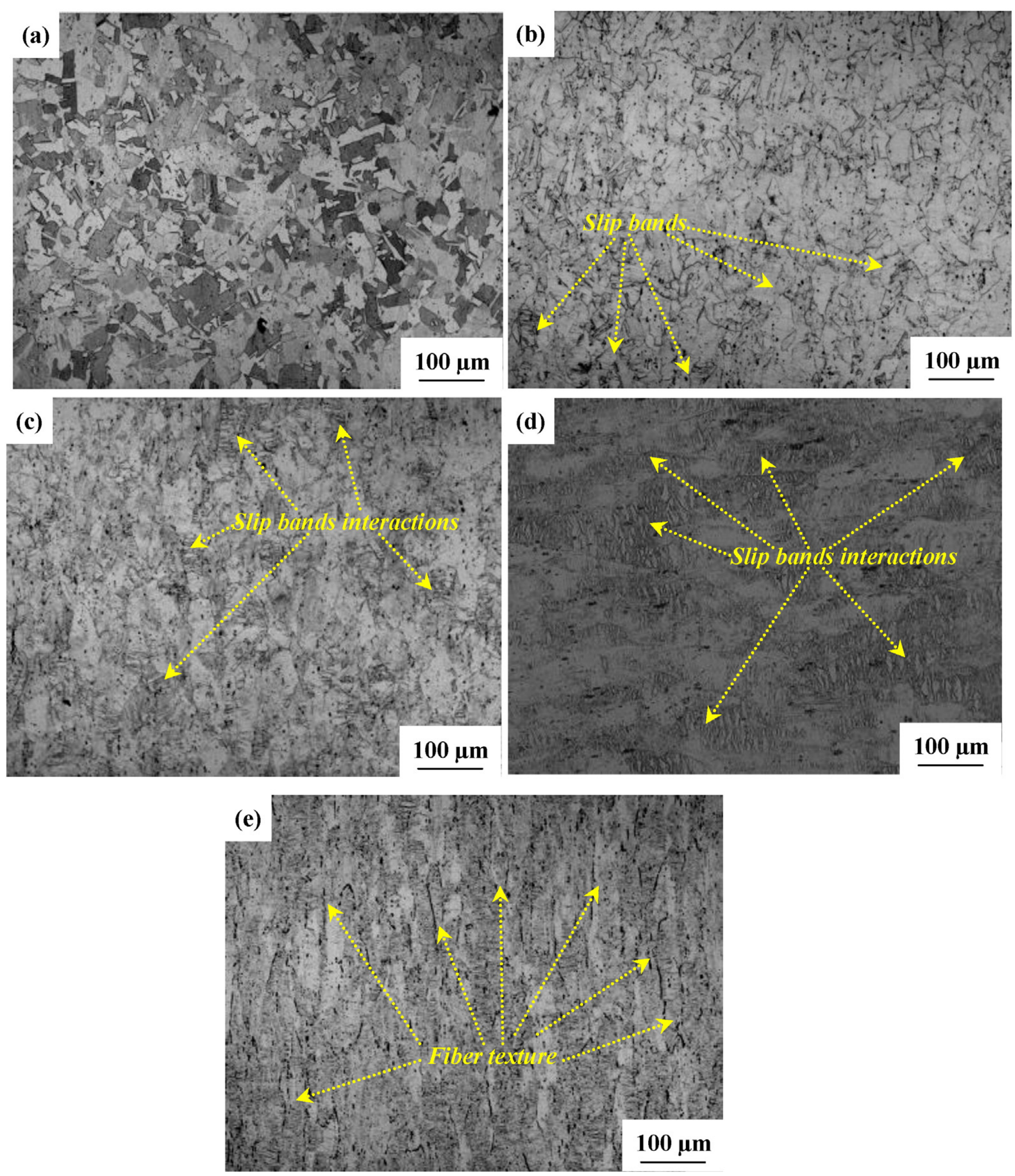

Fig. 2. Metallographic structure of the austenitic stainless steel before and after cryorolling: (a) the original austenite structure; (b) after 30% deformation; (c) after 50% deformation; (d) after 70% deformation; (e) after 90% deformation.

etching using the chromic acid solution with the 3 V applied voltage. For the TEM study, mechanically thinned 50 μm discs were prepared using twin gun precision ion polishing system (Gatan, model 691). X-ray diffraction (XRD) experiments were carried out using the D8 ADVANCE X-ray diffractometer. The tube voltage and current were 35 kV and 40 mA, respectively. The tube anode was CuKα1 ($\lambda = 0.15406$ nm), and the X-ray beam diameter was about 2 mm. The scan rate was 0.02°/s with 1 s per step. Microhardness was measured using the MH-3 Vickers microhardness tester with 200 g normal load and 10 s holding time on the as-polished regions. An average microhardness value was determined based on 5 indentation measurements. Mini-tensile test specimens with a gage length of 10 mm, 2.5 mm wide and 0.51 mm thick were prepared along the longitudinal direction, considering that the steel sheet was elongated along the longitudinal direction during rolling, as shown in Fig. 1. The mini-tensile test was conducted on the Instron 5948R micro material testing machine, with a chuck moving velocity of 0.1 mm/min. The morphology of the fracture surfaces was observed using JSM-5610LV SEM, operated at 20 kV.

3. Results

3.1. Microstructure

Fig. 2 shows optical micrographs of the Fe–25Cr–20Ni steel before and after cryorolling. It can be seen that the degree of grain deformation increases with the strain. A single austenite phase with homogeneous microstructure and obvious grain boundaries before deformation is observed, and the grain size is about 60 μm, as seen in Fig. 2a. After 30% deformation, in Fig. 2b, a small amount of slip bands is found in the austenite grain, which has also been observed in brass after cryorolling by Kumar et al. [13]. As the strain increases to 50%, the number of slip grains increases rapidly, and the slip bands in the grain are along the rolling direction, found in Fig. 2c. With further increasing the strain to 70%, the grain appearance changes greatly and most austenite grains exist in the form of long strips or flats. Meanwhile, obvious interactions occur between the adjacent slip bands and the original grain is refined, as seen in Fig. 2d. At the time, when the strain reaches 90% in Fig. 2e, the grain boundaries become blurred and the grains are elongated, contributing to the fiber texture formation.

X-ray diffraction patterns of the specimens before and after cryorolling are shown in Fig. 3. New diffraction peaks are not found after cryorolling, compared with the samples without deformation, indicating that the deformation-induced martensitic transformation did not occur in the Fe–25Cr–20Ni austenitic stainless steel during cryorolling. Meanwhile, the diffraction peaks of the samples after cryorolling become broader, probably due to the large residual stress in the samples after cryorolling. The full width at half maximum ($FWHM_{(111)}$) of the Fe–25Cr–20Ni steel increases from 0.324 (before cryorolling) to 0.388 and 0.424 when the deformation increases to 30%, 50%, respectively. With further strain increase peaks broadening becomes more obvious. The $FWHM_{(111)}$ increases from 0.456 to 0.496 with the increase of the deformation from 70% to 90%, which is increased by 40.7% and 53.1%, respectively compared with the samples without deformation. This is mainly due to the interaction of large residual stress and grain refinement after cryorolling [14]. A similar phenomenon was observed in pure Zr after cryorolling by Zhang et al. [15].

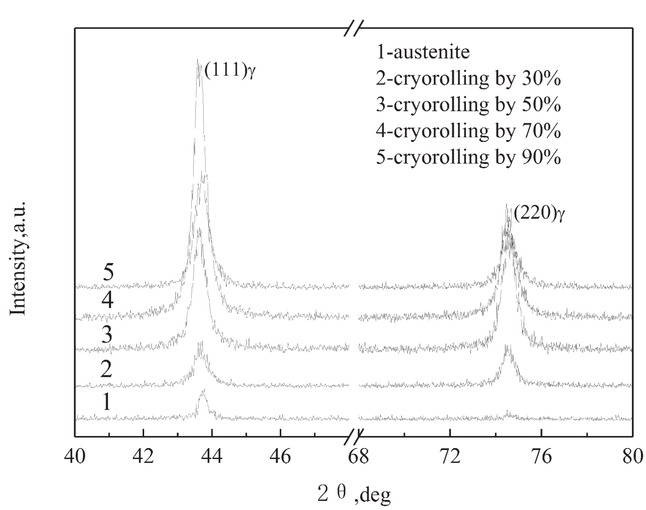

Fig. 3. Changes of XRD peak positions of the austenitic stainless steel before and after cryorolling.

Fig. 4 shows the microstructure of austenitic stainless steel at different degrees of deformation after cryorolling. It can be seen that at the initial deformation stage (30% strain), due to the dislocations motion, lots of dislocation lines are produced and high density tangled dislocations are observed in Fig. 4a. The motion of the dislocations was blocked, causing stress concentration in local regions. Thus, some deformation twins were formed. The number of deformation twins increased as the deformation increased to 50%. The distance between twins became smaller, and an interaction between the twins and the dislocations started to happen, as seen in Fig. 4b. By further increasing the strain to 70%, more twins were observed with a decrease of thickness owing to an increased plastic strain [16]. It is interesting to note that inside the twin–matrix lamellae, high density dislocations exist and lamellae are further refined by dislocation arrays or walls. As shown in Fig. 4c, several dislocation walls (as marked with arrows), roughly perpendicular to the twin boundaries, are formed in the lamellae [17]. Meanwhile, twin–twin intersections in different directions formed rhombic blocks with the 50–70 nm size, as seen in Fig. 4d. As the strain reached 90%, the grains of austenitic stainless steel refined to the nanometer scale, as seen in Fig. 4e (bright-field image), and f (dark-field image). The selected area electron diffraction pattern (SAED) of the samples after 90% deformation is shown in Fig. 4g. The corresponding ring pattern shown in Fig. 4g clearly points out that the average grain size is at the nanometer level (<100 nm). The SAED patterns showing diffraction rings are typical for polycrystals dominated by large misorientation angles [18]. Fig. 4h shows statistical grain size distribution of Fig. 4e and f. It can be clearly seen that there are plenty of nano-grains in the 90% cryorolled samples and the average grain size is about 20 nm.

Therefore, the strain accumulation resulted in different microstructure. During cryorolling, the dynamic recovery of dislocations was restrained by the deformation, leading to the formation of many dislocations. The dislocation density increased and high density tangled dislocations were formed with more deformation. Local stress concentration occurred once the dislocation movement was hindered, and the deformation twins continued to coordinate severe plastic deformation. When the strain is low, the plastic deformation was in the form of dislocation propagation and slip, while mechanical twinning became the main plastic deformation mode at high strain. By further increasing the strain, development of high-density mechanical twins leads to the reduction of the thickness of the corresponding matrix down to the nanometer scale, as seen in Fig. 4c and d. Apparently, formation of high-density twins introduced a large amount of twin boundaries that subdivide the original coarse grains into twin–matrix lamellae. With strain increasing, dislocation activities become functional inside the twin–matrix lamellae for accommodating further plastic deformation when formation of mechanical twins becomes more difficult within the thin lamellae. For minimizing the strain energy, dislocations in the thin twin–matrix lamellae arrange themselves into dislocation walls. As strain increases further, formation of sub-boundaries originating from the dislocation walls subdivides twin–matrix lamellae into nanometer-sized blocks with misorientations [19,20].

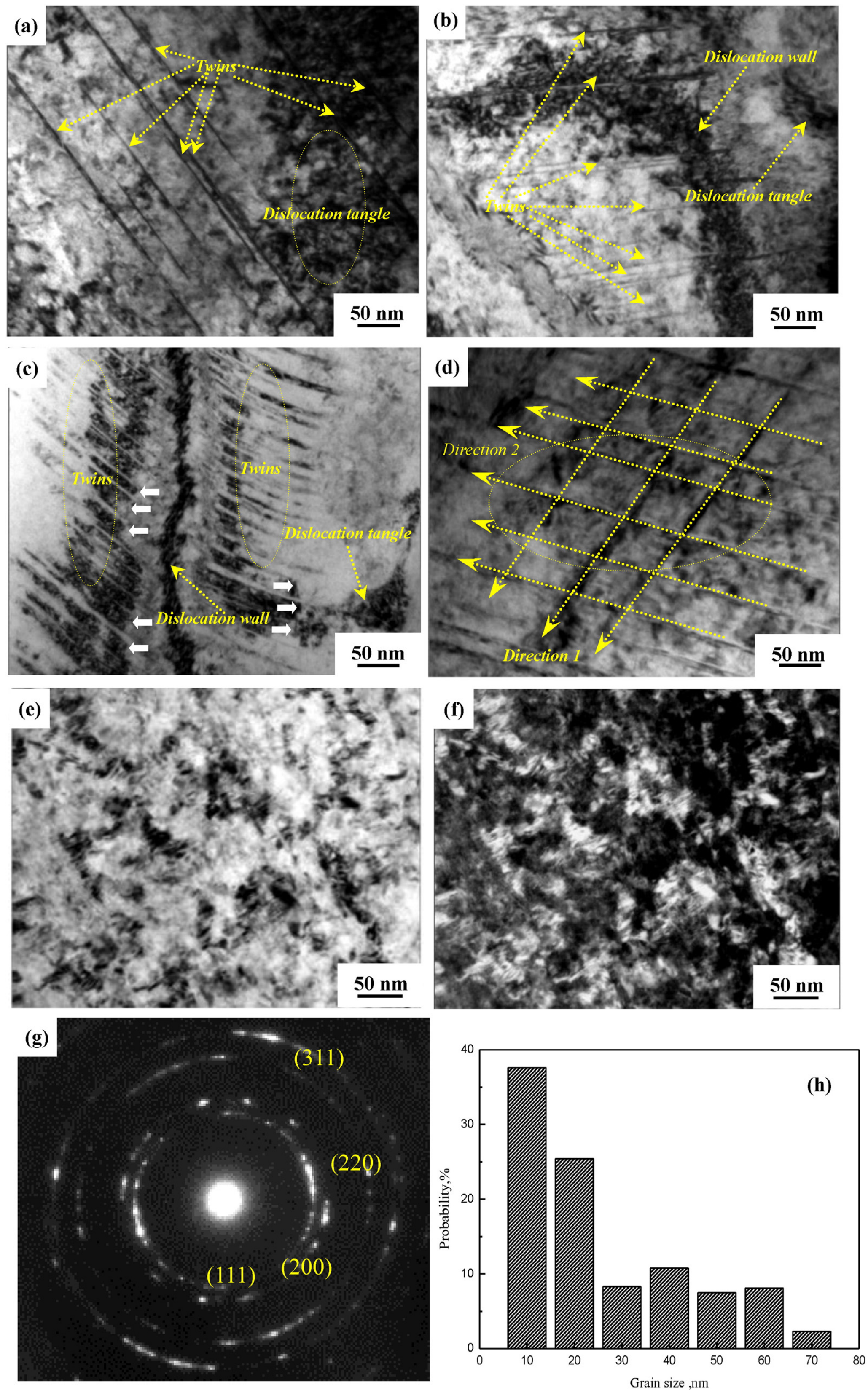

Fig. 4. Microstructure of the austenitic stainless steel at different degrees of deformation after cryorolling: (a) after 30% deformation; (b) after 50% deformation; (c) and (d) after 70% deformation, showing the formation of dislocation walls (as indicated by arrows) inside the twin lamellae; (e) and (f) after 90% deformation; (g) the corresponding selected-area electron diffraction of Fig. 4e and f; (h) statistical grain size distribution of Fig. 4e and f.

3.2. Mechanical properties

The microhardness of the original austenitic stainless steel was 260 HV. The microhardness increased to 410 HV for the 30% cryorolled samples (Fig. 5). By further increasing the deformation to 50%, the microhardness increased by 10.5%, from 410 HV to 453 HV. The microhardness enhanced to 497 HV upon further deformation of 70%. The maximum reduction in area achieved by the cryorolling was 90% with the corresponding microhardness value of 520 HV. The hardness improved by 100% compared with the original un-deformed sample. The results are in agreement with Milad et al. [21], but contradict Kain et al. [22]. It can be seen that the hardness enhancement is mainly due to the grain size effect and accumulation of large plastic strain achieved by cryorolling. Rolling of metals and alloys at cryogenic temperatures suppresses dynamic recovery and recrystallization [23], leading to high dislocation density. Thus, at the initial deformation stage, microhardness of the samples increases rapidly because of the work hardening. With further increase in the strain, the density of accumulated dislocations reaches its highest saturation level and the interactions of the dislocations are significantly enhanced, giving rise to the formation of large amounts of deformation twins in the austenite structure, which is beneficial for the grain refinement. Therefore, hardness increases due to the strain hardening, along with the grain size reduction during cryorolling [24].

Fig. 6 shows the engineering stress–strain curves from the mini-tensile tests of the austenitic stainless steel before and after cryorolling. The un-deformed sample shows low yield strength of about 305 MPa and the tensile strength of about 645 MPa. The yield strength and tensile strength increased to 568 MPa and 994 MPa for the 30% cryorolled samples. After 50% deformation, the yield strength and tensile strength greatly increase to approximately 1380 MPa and 1441 MPa. As the strain reached 70%, the yield strength and the tensile strength increased slightly to about 1460 MPa and 1514 MPa, respectively. By further increasing the strain to 90%, the yield strength reached 1502 MPa and the tensile strength reached 1560 MPa, which is respectively 4.9 and 2.4 times higher than the un-deformed sample. The increase of the strength tends to be smooth. Therefore, the yield strength and the tensile strength of the samples increased with deformation. When the strain increased to 50%, the strength increased drastically, however, with further increase of the strain, the strength increased slightly and became stable. From Fig. 6, it can be also seen that the elongation follows a path opposite to that of the strength. The elongation of the primary sample is 40.8%. After 30% and 90% deformation, the elongation of the samples decreased to 14.8% and 6.4%, respectively. The relation between the Vickers hardness and the ultimate tensile strength at different locations after rolling obeys the empirical formula, where the Vickers hardness value is about 1/3 of the ultimate tensile strength value [25]. The corresponding ratio of yield strength to tensile strength increases from 0.47 (no deformation) to 0.96 (90% deformation), and as the deformation increases over 50%, the ratio of yield strength to tensile strength is almost unchanged and remains at 0.96. This is different from the austenitic stainless steel with the metastable microstructure, where the ratio of yield strength to tensile strength increases significantly with strain due to the deformation-induced martensitic transformation. However, the deformation-induced martensitic transformations did not occur in the Fe–25Cr–20Ni austenitic stainless steels during cryorolling. Thus, as the deformation increased to some extent, the ratio of yield strength to tensile strength became stable. With the increase of the deformation, the dislocation proliferation was aggravated, which lead to the formation of the high density tangled dislocations. As a result, the dislocation motion was hindered. Meanwhile, as the deformation rose, a large number of deformation twins appeared in the grains and the interaction between the twins and the dislocations was significantly enhanced, contributing to the grain refinement. Thus, the strength of the samples increased, while the elongation decreased with larger deformation.

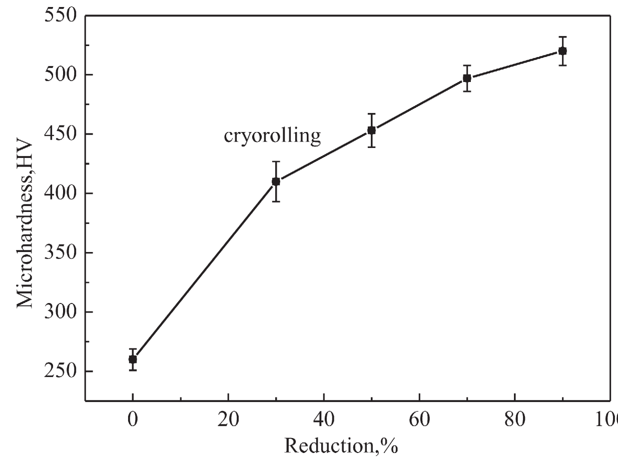

Fig. 5. Relationship between the microhardness and the cryorolling deformation.

The fracture surfaces morphology of the austenitic stainless steel before and after cryorolling is shown in Fig. 7. Fig. 7a shows the fracture surface of the original austenitic stainless steel, which is typical ductile fracture. Many large and deep dimples with the average size of about 8 μm can be found. In Fig. 7b, after cryorolling with 30% deformation, the number of large and deep dimples decreased and the average size of the dimples was about 6 μm. When the deformation increased to 50%, the size and number of the dimples decreased further with the average size of about 4 μm, found in Fig. 7c. As seen in Fig. 7d, by further increasing the deformation to 70%, only a small amount of large and deep dimples can be observed and the average size decreased to about 3 μm, showing quasi-cleavage fracture characteristics in the local area. When the deformation reached 90%, the sample fracture surface was smooth and the cleavage surface could be observed in most regions. Meanwhile, many small and shallow dimples with the size less than 1 μm can be found in other areas, as seen in Fig. 7e. This indicates that the austenitic grain of the austenitic stainless steel can be obviously refined after cryorolling and the grain size was refined to the nanometer scale with higher deformation. Compared with the original austenitic stainless steel structure, the plasticity of the austenitic stainless steel apparently decreased after cryorolling and the fracture morphology transformed from typical ductile to a mixture of quasi-cleavage and ductile fracture. Similar phenomenon was observed in fractographs of the high nitrogen austenite stainless steel after cold compression by J.H. Shin and J.W. Lee' [26].

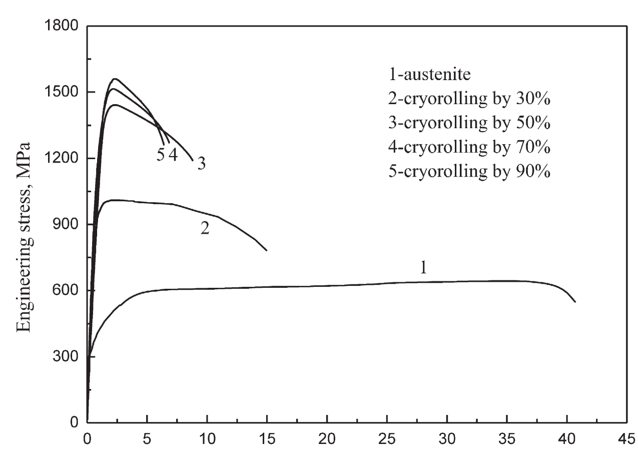

Fig. 6. Engineering stress–strain curves of the mini-tensile sample before and after cryorolling.

4. Discussion

It is well known that mechanical twinning and dislocation slip are the dominant plastic deformation mechanisms, which depend on the stacking fault energy (SFE). The materials with high SFE deform by means of dislocations movement, while materials with low SFE deform by mechanical twinning. Under the experimental conditions, the SFE of the Fe–25Cr–20Ni austenitic stainless steel is calculated to be 43.8 mJ/m^2, according to the following empirical formula [27]:

$$\mathrm{SFE}\ [\mathrm{mJ/m^2}] = 25.7 + 2\mathrm{Ni} + 410\mathrm{C} - 0.9\mathrm{Cr} - 77\mathrm{N} - 13\mathrm{Si} - 1.2\mathrm{Mn}. \quad (1)$$

Considering the effect of the Nb alloying element, the SFE of the Fe–25Cr–20Ni austenitic stainless steel is over 43.8 mJ/m^2, which is much higher than that of the AISI 304, AISI 301, AISI316 and AISI 201 austenitic stainless steels [28]. Thus, the microstructure change of the Fe–25Cr–20Ni austenitic stainless steel during cryorolling is different from the austenitic stainless steel with lower SFE. Hadji [29] suggested that the deformation mechanism is closely related to the SFE of austenite. For the lower SFE values (the case of 304 stainless steel), a mixture of ε-martensite and mechanical twins appear as intermediate phases before the formation of the α phase. Upon increasing the SFE values (the case of 316 stainless steel), mechanical twinning becomes the dominant deformation mode, and no ε-martensite is detected in this steel. However, Morikawa's [30] showed that in face centered cubic (fcc) pure metals with a high SFE, such as aluminum, the prominent structures are dense dislocation walls and micro bands, while, in fcc alloys with low SFE, such as α-brass, deformation twinning has an important role. After cold rolling dense twin matrix lamellar structure develops, which is then destroyed by the shear bands forming the fine-grained structure. Sarma [31] studied the effects of SFE on fcc metals after cryorolling, such as Al, AA6061, Cu, Cu–4.6 at.%Al, Cu–9 at.%Al and Cu–15 at.%Al. The results showed that high SFE metals deformed by dislocation slip and low SFE metals deformed by twinning during cryogenic temperature (CT) rolling and room temperature (RT) rolling. Metals with intermediate SFEs deformed by twinning during CT rolling, but by dislocation slip during RT rolling. This makes CT rolling more effective than the RT rolling in terms of the strength enhancement.

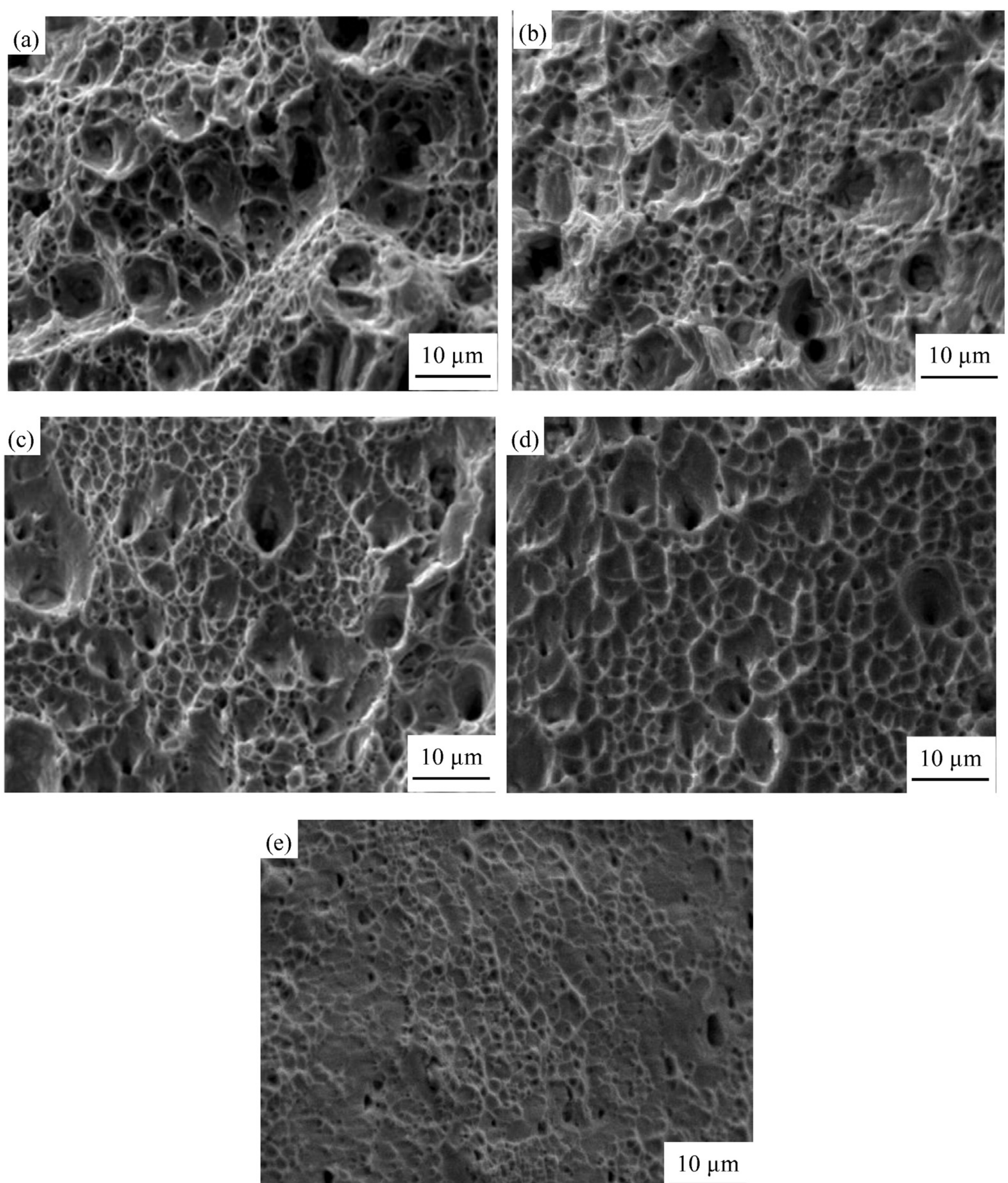

Fig. 7. Fracture surface morphology of the austenitic stainless steel before and after cryorolling: (a) original austenite structure; (b) after 30% deformation; (c) after 50% deformation; (d) after 70% deformation; (e) after 90% deformation.

Present experiments provide impressive support for the Sarma's results. Under low deformation conditions (30% deformation), the microstructure is mainly high density tangled dislocations with a small amount of mechanical twins, seen in Fig. 4a. With increasing the deformation to 70%, the microstructure turns to a large amount of mechanical twins, dislocation walls and dislocation tangles. Meanwhile, the interaction between the twins is significantly enhanced, leading to the formation of the nanometer-sized rhombic blocks, as seen in Fig. 4c and d. By further increasing the deformation to 90%, the austenite grain is fully refined to the nanometer scale, which can be also found in the SAED pattern of Fig. 4g, showing clear and uniformly continuous diffraction ring pattern. In summary, the SFE of the Fe–25Cr–20Ni austenitic stainless steel belongs to medium SFE, which is between high SFE and low SFE. Therefore, dislocation slip and mechanical twins are the dominant models to coordinate the heavy deformation during cryorolling, which is consistent with the results in Ref. [31].

In terms of the experimental observations and analyses, the grain refinement mechanism in the Fe–25Cr–20Ni stainless steel as a function of cryorolling deformation can be summarized as follows. (i) In the low strain region, lots of dislocation lines are produced and a small amount of mechanical twins occur in the austenite grain. (ii) With further strain increase, the interaction of high density dislocations results in the formation of dislocation tangles and dislocation walls. Meanwhile, large amounts of mechanical twins are formed and the formation of a high density of mechanical twins subdivides the original coarse grains into twin–matrix lamellae. (iii) In the high strain region, development of dislocation arrays and twin–twin intersections further subdivide the twin–matrix lamellae into nanometer-sized blocks. (iv) These nanometer-sized blocks evolve into randomly oriented nanocrystallites. Formation of randomly orientated nanocrystallites requires a substantial variation in the related orientations of these nanometer-sized blocks (Fig. 4d). Possible mechanisms responsible for the formation of random orientations may involve in grain boundary sliding and/or grain rotation. When the grain size is reduced down to the nanometer range, the grain rotation and grain boundary sliding will be much easier compared with the coarse ones [32]. Grain rotation is an alternative process accommodating plastic deformation of nanocrystallites, which may effectively increase the misorientations and result in the formation of randomly orientated nanocrystallites [33].

5. Conclusions

The microstructure and mechanical properties of the Fe–25Cr–20Ni austenitic stainless steels after cryorolling with different reductions were systematically characterized and analyzed. The results are as follows:

1. With the increase of the deformation, the austenite grains were elongated along the rolling direction and appeared in the form of long strips or flats. At the time when the deformation reached 90%, the grain boundaries became blurred and the fiber texture was formed. The diffraction peaks of the Fe–25Cr–20Ni austenitic stainless steel became broader with the strain increase.
2. The dynamic recovery of dislocations was restrained by cryorolling. After 30% deformation, high density tangled dislocations and a small amount of deformation twins appeared in the steels. After 50% deformation, the number of deformation twins increases, and the distance between twins becomes smaller, and the interaction between the twins and the dislocations starts to happen. With the increase of the deformation to 70%, a large amount of deformation twins was produced and the interaction between the twins and the dislocations was significantly enhanced. When the deformation was 90%, the grain size was fully refined to the nanometer scale.
3. The microhardness and the strength of the austenitic stainless steels increased with the rolling deformation. The yield strength and the ultimate strength increased from 305 MPa and 645 MPa (no deformation) to 1502 MPa and 1560 MPa (90% deformation), respectively. During the initial deformation stage, the strength drastically increased. However, with further increase of the deformation, the strength increased only slightly and became stable. The corresponding elongation decreased from 40.8% to 6.4%. The tensile fracture morphology changed from typical dimple rupture to a mixture of quasi-cleavage and ductile fracture. The microhardness increased with the deformation. After 90% deformation, the microhardness was 520 HV, which is a 100% increase, compared with the original un-deformed sample.

Acknowledgments

This work was supported by the National Natural Science Foundation of China under grants no. 50801021 and 51201061, and by the Program for the Young Key Teachers in the Henan Province under grant no. 2011GGJS-070, the Henan Province Program for Science and Technology Innovation Excellent Talents (144200510009), the Science and technology project of Henan Province (152102210077), and the Science and Technology Innovation Team of Henan University of Science and Technology (2015XTD006).

References

[1] A. Hedayati, A. Najafizadeh, A. Kermanpur, F. Forouzan, The effect of cold rolling regime on microstructure and mechanical properties of AISI 304L stainless steel, J. Mater. Process. Tech. 210 (2010) 1017–1022.
[2] J.X. Huang, X.N. Ye, Z. Xu, Effect of cold rolling on microstructure and mechanical properties of AISI 301LN metastable austenitic stainless steels, J. Iron Steel Res. Int. 19 (2012) 59–63.
[3] K.M. Chen, C.C. Zheng, Z.Z. Yuan, J.Z. Lu, X.D. Ren, X.M. Luo, Deformation microstructures of austenitic stainless steel 2Cr13Mn9Ni4 under ultrafast stain rate by laser shock processing, Mater. Sci. Eng. A 587 (2013) 244–249.
[4] P. Behjati, A. Kermanpur, A. Najafizadeh, H.B. Samaei, Microstructural investigation on deformation behavior of high purity Fe–Cr–Ni austenitic alloys during tensile testing at different temperatures, Mater. Sci. Eng. A 618 (2014) 16–21.
[5] E. Mostafa, Z.H. Abbas, R.A. Hamid, An investigation into the room temperature mechanical properties of nanocrystalline austenitic stainless steels, Mater. Des. 45 (2013) 674–681.
[6] I. Shakhova, V. Dudko, A. Belyakov, K. Tsuzaki, R. Kaibyshev, Effect of large strain cold rolling and subsequent annealing on microstructure and mechanical properties of an austenitic stainless steel, Mater. Sci. Eng. A 545 (2012) 176–186.
[7] Y.M. Wang, M.W. Chen, F.H. Zhou, E. Ma, High tensile ductility in a nanostructured metal, Nature 419 (2002) 912–917.
[8] T.R. Lee, C.P. Chang, P.W. Kao, The tensile behavior and deformation microstructure of cryo-rolled and annealed pure nickel, Mater. Sci. Eng. A 408 (2005) 131–135.
[9] N. Rangaraju, T. Raghuram, B.V. Krishna, K. Rao, P. Venugopal, Effect of cryorolling and annealing on microstructure and properties of commercially pure aluminum, Mater. Sci. Eng. A 398 (2005) 246–251.
[10] K. Youssef, M. Sakaliyska, H. Bahmanpour, R. Scattergood, C.C. Koch, Effect of stacking fault energy on mechanical behavior of bulk nanocrystalline Cu and Cu-alloys, Acta Mater. 59 (2011) 5758–5764.
[11] S.V. Zherebtsov, G.S. Dyakonov, A.A. Salem, V.I. Sokolenko, G.A. Salishchev, S.L. Semiatin, Formation of nanostructures in commercial-purity titanium via cryorolling, Acta Mater. 61 (2013) 1167–1178.
[12] S.V. Subramanya, K. Sivaprasad, D. Strum, M. Heilmaier, Microstructure and mechanical properties of ultrafine grained Cu–Zn and Cu–Al alloys produced by cryorolling and annealing, Mater. Sci. Eng. A 489 (2008) 253–258.
[13] R. Kumar, S.M. Dasharath, P.C. Kang, C.C. Koch, S. Mula, Enhancement of mechanical properties of low stacking fault energy brass processed by cryorolling followed by short-annealing, Mater. Des. 67 (2015) 637–643.
[14] G. Sunkulp, K. Nachiket, R. Jayaganthan, I.V. Singh, D. Srivastava, G.K. Dey, N. Saibaba, Mechanical behaviour and microstructural characterizations of ultrafine grained Zircaloy-2 processed by cryorolling, Mater. Sci. Eng. A 603 (2014) 23–29.
[15] D.F. Guo, M. Li, Y.D. Shi, Z.B. Zhang, T.Y. Ma, H.T. Zhang, X.Y. Zhang, Simultaneously enhancing the ductility and strength of cryorolled Zr via tailoring dislocation configurations, Mater. Sci. Eng. A 558 (2012) 611–615.
[16] J.Z. Lu, K.Y. Luo, Y.K. Zhang, G.F. Sun, Y.Y. Gu, J.Z. Zhou, X.D. Ren, X.C. Zhang, L.F. Zhang, K.M. Chen, C.Y. Cui, Y.F. Jiang, A.X. Feng, L. Zhang, Grain refinement mechanism of multiple laser shock processing impacts on ANSI 304 stainless steel, Acta Mater. 58 (2010) 5354–5362.
[17] K. Wang, N.R. Tao, G. Liu, J. Lu, K. Lu, Plastic strain-induced grain refinement at the nanometer scale in copper, Acta Mater. 54 (2006) 5281–5291.
[18] H. Ueno, K. Kakihata, Y. Kaneko, S. Hashimoto, A. Vinogradov, Enhanced fatigue properties of nanostructured austenitic SUS 316L stainless steel, Acta Mater. 59 (2011) 7060–7069.
[19] N.R. Tao, H.W. Zhang, J. Lu, K. Lu, Development of nanostructures in metallic materials with low stacking fault energies during surface mechanical attrition treatment (SMAT), Mater. Trans. 44 (2003) 1919–1925.

[20] N.R. Tao, X.L. Wu, M.L. Sui, J. Lu, K. Lu, Grain refinement at the nanoscale via mechanical twinning and dislocation interaction in a nickel-based alloy, J. Mater. Res. 19 (2004) 1623–1629.
[21] M. Milad, N. Zreiba, F. Elhalouani, C. Baradai, The effect of cold work on structure and properties of AISI 304 stainless steel, J. Mater. Process. Tech. 203 (2008) 80–85.
[22] V. Kain, K. Chandra, K.N. Adhe, P.K. De, Effect of cold work on low-temperature sensitization behaviour of austenitic stainless steels, J. Nucl. Mater. 334 (2004) 115–132.
[23] D. Singh, P.N. Rao, R. Jayaganthan, Effect of deformation temperature on mechanical properties of UFG Al–Mg alloys processed by rolling, Mater. Des. 50 (2013) 646–655.
[24] P.N. Rao, D. Singh, R. Jayaganthan, Effect of post cryorolling treatments on microstructural and mechanical behaviour of ultrafine grained Al–Mg–Si alloy, J. Mater. Sci. Technol. 30 (2014) 998–1005.
[25] Compilations group of “Mechanical property of metal”, Mechanical property of metals, Mechanical Industry Press, Beijing, 1982: 230 (in Chinese).
[26] J.H. Shin, J.W. Lee, Effects of twin intersection on the tensile behavior in high nitrogen austenitic stainless steel, Mater. Charact. 91 (2014) 19–25.
[27] F. Pickering, Conference of Stainless Steels, GoteborgThe Institute of Metals, London 1985, p. 2.
[28] F.Y. Dong, P. Zhang, J.C. Pang, D.M. Chen, K. Yang, Z.F. Zhang, Optimizing strength and ductility of austenitic stainless steels through equal-channel angular pressing and adding nitrogen element, Mater. Sci. Eng. A 587 (2013) 185–191.
[29] M. Hadji, R. Badji, Microstructure and mechanical properties of austenitic stainless steels after cold rolling, J. Mater. Eng. Perform. 11 (2002) 145–151.
[30] T. Morikawa, K. Higashida, The role of deformation twinning in the formation of a fine-grained structure in cold-rolled 310 steels, J. Mater. Sci. 41 (2006) 2581–2585.
[31] V.S. Sarma, J. Wang, W.W. Jian, A. Kauffmann, H. Conrad, J. Freudenberger, Y.T. Zhu, Role of stacking fault energy in strengthening due to cryo-deformation of FCC metals, Mater. Sci. Eng. A 527 (2010) 7624–7630.
[32] H.V. Swygenhoven, D. Farkas, A. Caro, Grain-boundary structures in polycrystalline metals at the nanoscale, Phys. Rev. B 62 (2000) 831–838.
[33] E. Hellstern, H.J. Fecht, Z. Fu, W.L. Johnson, Structural and thermodynamic properties of heavily mechanically deformed Ru and AlRu, J. Appl. Phys. 65 (1989) 305–310.